Metrological Characterization of a Vision-Based Measurement System for the Online Inspection of Automotive Rubber Profile

Rosario Anchini, Giuseppe Di Leo, Consolatina Liguori, *Member, IEEE*, and Alfredo Paolillo, *Member, IEEE*

***Abstract*—This paper deals with the metrological characterization of a stereovision-based measurement system for the inspection of automotive rubber profiles in an industrial plant. The characterization of this class of measurement systems introduces new challenges due to both the unavailability of reference measurement instruments and the complexity of the measurement system itself, which does not allow a straightforward application of the standard procedures for uncertainty evaluation. To assign optimum values to a number of design parameters, the followed approach focuses not only on evaluating the total uncertainty but also on analyzing systematic effects and influence quantities.**

***Index Terms*—Automotive profile, contactless measurement, image processing, machine vision, uncertainty evaluation.**

I. Introduction

TODAY'S industry is very much attracted to the possibilities offered by image-based measurement systems [1]–[6] for product inspection. Traditional areas where these have been successful are the no-contact inspection of manufactured goods such as automobiles, semiconductor chips, food, and pharmaceuticals. The goal is to reduce production costs due to manual labor or defective parts and to ensure consistent product quality. Image-based systems can automate manufacturing processes by controlling manufacturing equipment such as industrial robotic arms. They may also allow manufacturers to reduce spending on defective goods in that they are useful for checking for defects one by one. The aim here is to correct the parameters of the industrial process as soon as a defect is found, for example, in silicon wafers, semiconductor chips, or painted vehicle surfaces. Machine vision systems have also taken on an important role for mechanical or stamped metal components in measuring all parts produced to ensure that they fall within given specification limits. The key to their success can be found in their distinctive attributes such as flexibility, reliability, higher operating speeds, consistency, and objectivity, which have made them competitive compared with traditional measurement systems. However, when reporting measurement results, in almost every case, uncertainty or doubt about correctness is ignored, although it should be obligatory for some quantitative indication of the quality of each result to be given. Moreover, there should be a univocal approach to the definition and evaluation of uncertainty. In the absence of this, no universally assessed reliability can be attributed to measured data, nor can a serious comparison of the stated result be made against a reference value or specification limits. There is justification, then, for making efforts to address the issue of giving methods for providing quantitative indications of result uncertainties. This task could be accomplished through suitable parameters such as accuracy, which is frequently adopted for characterizing an optical measuring system, although its definition is not universally accepted [7], [8]. Finally, the evaluation of accuracy for optical 3-D measurement imaging systems may be carried out in terms of the following errors defined in VDI/VDE 2634/part 2 [9]: quality parameter probing, sphere spacing, and flatness measurement.

Some considerations can be made about the procedures followed to determine the parameters presented above. Most of the methods proposed are based on the use of reference objects, that is, 2-D or 3-D arrangement of features whose geometric attributes have been measured through high-precision procedures, but the proposed approaches are not universally defined. Instead, the *Guide to the Expression of Uncertainty in Measurement* (GUM), which has been published by the International Organization for Standardization (ISO) [10], standardizes the measurement quality expression, defining uncertainty as "a parameter associated with the result of a measurement that characterizes the dispersion of the values that could reasonably be attributed to the quantity to be measured." The uncertainty completely describes the measurement reliability if the result is corrected for all known systematic effects that significantly influence the estimation. Systematic errors arising from recognized effects of influence quantities on the measurement result have to be quantified, and then, a correction must be evaluated and applied. The uncertainty u of the corrected result depends on the variability of the measurements and on the uncertainty of the correction itself.

A straightforward application of the uncertainty evaluation procedure to image processing-based measurements, as suggested by GUM, may be difficult to follow. In this framework, to determine an analytical model of u and its relationships with influence and measurement parameters, the authors have proposed an indirect (type B [10]) "white-box" approach [11],

Manuscript received September 14, 2007; revised March 4, 2008. First published October 3, 2008; current version published December 9, 2008. The Associate Editor coordinating the review process for this paper was Prof. Alessandro Ferrero.

The authors are with the Department of Electrical and Information Engineering (DIIIE), University of Salerno, 84084 Saleno, Italy (e-mail: tliguori@unisa.it).

Color versions of one or more of the figures in this paper are available online at http://ieeexplore.ieee.org.

Digital Object Identifier 10.1109/TIM.2008.2004979

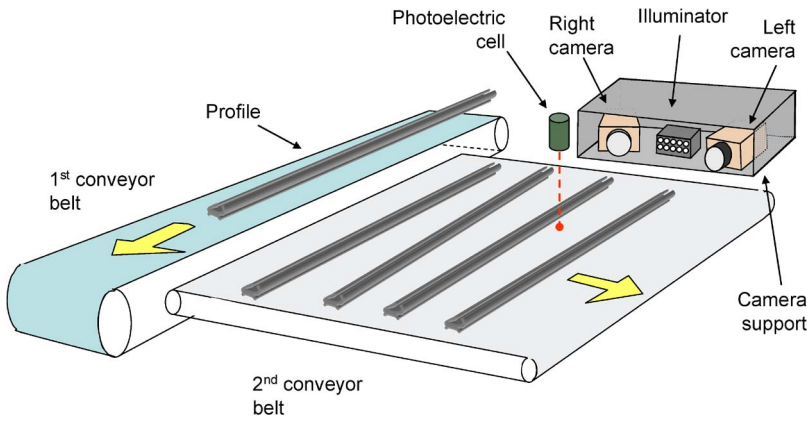

Fig. 1. Hardware structure of the application.

[12]. These relationships allow u to be foreseen for almost all possible types of the following: operating conditions (for example, with vibrations, flickering lights, and irregular background), measurement parameters (for example, with different focus and shutter settings), and image processing software options. Consequently, they can be used for driving the design of the image-based measurement system.

However, this solution also has a number of limits and drawbacks, as follows.

1) The causes of uncertainty and deterministic error must be known and analytically modeled.
2) The image processing algorithms must be known to allow for the propagation of acquired image uncertainty via the measurement software, and propagation could become very complicated for a multipart software.
3) The values of influence parameters must be known, even if only roughly, so that they can be used as data input for evaluating u.

This paper deals with the metrological characterization of a measurement station for the online inspection of rubber profiles using stereovision. Because of the complexity of the measurement procedure and the environment where the system is operating, it is very difficult to apply the white box approach. Consequently, the metrological characterization is carried out by following a type-A [10] approach, which falls within traditional and well-known statistical methods. The issues experienced in the application of a type-A approach for the characterization of the system setup are quite general for any computer-vision-based measurement system. The solutions adopted here can, therefore, also be of use when characterizing other vision-based measurement systems, since the problems to be solved in characterizing such systems are often similar. Moreover, the tests carried out are used not only to evaluate measurement uncertainty but also to aid the final tuning of the measurement system.

In the following, after briefly summarizing the overall measurement station structure, the procedure implemented for measurement system characterization is presented, together with some experimental results. Furthermore, the effects of causes of uncertainty and influence quantities will be discussed, and their influences on final results will be quantified.

II. System Overview

The measurement system is currently operating on the extrusion lines at a Metzeler Automotive Profile Systems (APS) group plant. It is located at the end of each line, near a conveyor belt bench (Fig. 1). The hardware comprises digital IEEE-1394 cameras, each yielding from a different perspective angle a 2-D image of the leading transversal section of the profile. Since the surface of profiles is dark and poorly reflecting, a light-emitting diode (LED) illuminator lights up the profile section to increase the image contrast. A photoelectric cell detects the presence of a profile in front of the cameras and triggers image acquisition and processing via an acquisition board held in an expansion slot of the computing unit (PC).

The online operation of the measurement station can be viewed as a sequence of modules detailed in the following and shown in Fig. 2.

A. Image Acquisition

Two images are acquired by two Guppy F-080 IEEE-1394 standard cameras equipped with a 4.8-mm $\times$ 3.6-mm size sensor. The image size is 1024 $\times$ 768 pixels. Both lenses have a focal length of 16 mm, an F/number of 1:1.4, an iris range of [1.4, 16], and a minimum object distance of 25 mm. The illuminator comprises 12 white-light LEDs, each with a 550-nm peak wavelength and a luminous intensity of 2500 mcd.

B. 2-D Image Processing

For each of the two images, the same 2-D processing steps are applied to extract the contours of the rubber profile cross section. The localization of the cross section contour is a key task in the measurement procedure since final measurements are made on the 3-D reconstruction of the 2-D contours. The developed image processing algorithms apply a sequence of known image processing techniques: A histogram enhancement routine normalizes the grey-level distribution in the image; a region growing stage [4], [5], [13], [14] locates all the pixels belonging to the profile section (the foreground region); and a contour tracking algorithm locates the contour as the border of the foreground region. In particular, the region growing algorithm identifies, first, two sets of *seed pixels* for the two

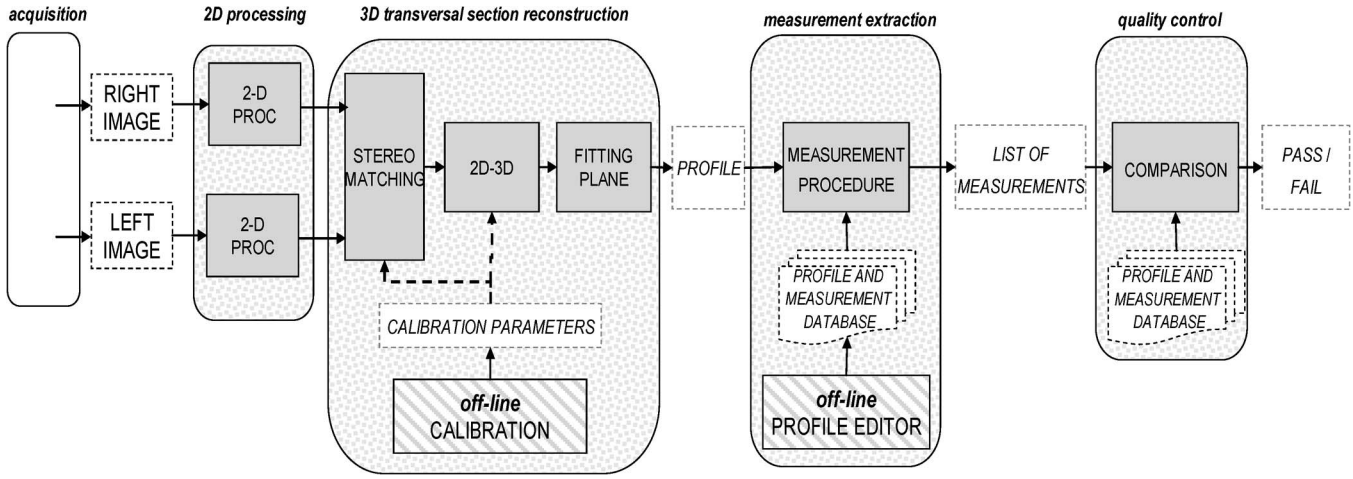

Fig. 2. Software architecture of the application.

classes via a simple thresholding. It then scans the image and classifies each pixel either into the *foreground* class or into the *background* class if it has, respectively, a *foreground* or a *background* neighboring pixel and if its value is close enough to this neighbor. The parameters of the 2-D processing stage, namely, the thresholds of the region growing and a few others related to the histogram enhancement, were fixed to the values that had experimentally and correctly processed all the different types of profiles.

C. 3-D Reconstruction

The two 2-D contours determined in the previous step are processed to obtain a 3-D reconstruction of the contours of the leading cross section. This module needs data that are determined offline during a calibration procedure (developed on the basis of the well-known procedure proposed by Zhang [15]). This requires the two cameras to observe a planar target whose geometry in 3-D space is known to a very good degree of precision, shown at a few different orientations (at least five). The target can freely be moved, and the motion does not need to be known. To obtain better accuracy ($\sim$10 μm), a sandblasted metal plate, shown in Fig. 3, containing a pattern of 6×5 square holes (120 square corners) is adopted as the target instead of the commonly adopted paper sheet printings. Estimating the corner positions in several pairs of images, which is achieved by suitably processing them, and knowing the target geometry in millimeters allows the parameters of the vision system to be calculated by means of a procedure based on the maximum likelihood criterion. A semiautomated procedure for corner detection in calibration images was implemented, which yields two pairs of 2-D image coordinates for each target corner [5], [13].

The actual 3-D reconstruction phase can be divided into the following two stages: 1) the search for matching stereo pairs, namely, the pair of image points in the left and right images generated by the same real point; and 2) the calculation of the 3-D coordinates of the profile contour points as a function of the two stereo pairs. The search for stereo pairs exhibits several difficulties in the case of rubber profiles, since their possible shapes are extremely changeable, and thus, no *a priori*

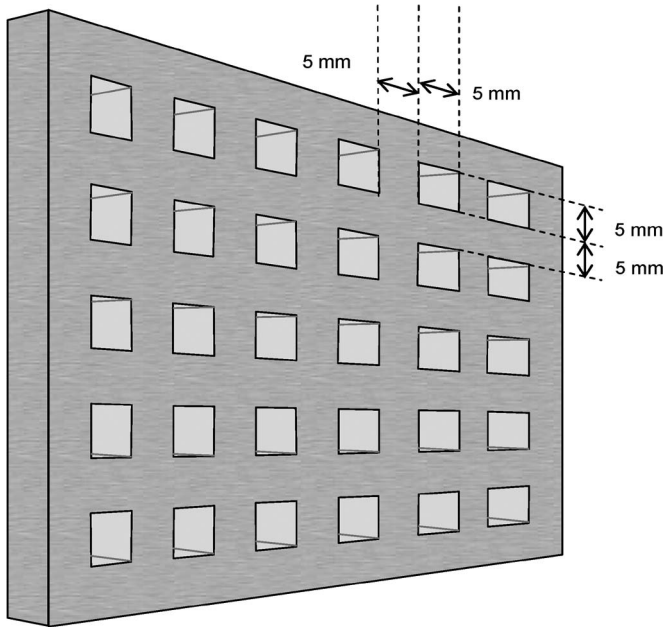

Fig. 3. Calibration target.

hypothesis can be made about the geometrical curve describing the profile. The proposed algorithm exploits the generally valid epipolar constraint [14], [16], which is basically that, given a point on one image (e.g., the left one), the corresponding point on the other (e.g., the right) image lies on a line (the so-called epipolar line), whose localization can be determined from the calibration parameters. The point on the right image that corresponds to a given point on the left image can be searched for within the intersections between its epipolar line and the profile contours.

However, due to the possible complex shapes of the section profiles, the actual matching point of the pair cannot reliably be discerned using the criteria known in the literature. Hence, a novel stereo-matching solution has been designed based on the localization of stereo pairs first on the contours of the convex hulls of the profiles in the two images. The convex hull of a 2-D set of points is the smallest convex polygon that includes the points. The advantage of the introduction of the convex hull is that there are always only two intersections between an epipolar

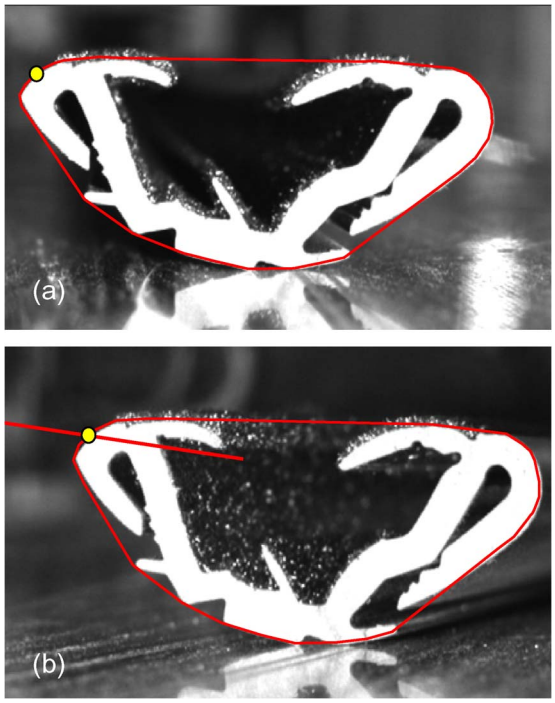

Fig. 4. Examples of convex hulls of the (a) left and (b) right images with two corresponding points and a piece of the right epipolar line.

line and the contour of a convex hull. The 3-D coordinates of the points of the 3-D profile convex hull can easily be determined using the procedure proposed in Fig. 4. The hypothesis that a 3-D reconstruction of a profile convex hull lies on the same plane as the profile itself allows one to state that the transformation that moves the left image convex hull onto the 3-D convex hull is the same transformation that moves the left profile onto the 3-D profile. Then, the parameters of this transformation (a linear rototranslation with rescaling of coordinates) are estimated by means of a fitting algorithm. Eventually, this transformation is applied to each point of the left-image contours to achieve the 3-D representation of the whole profile. To simplify the subsequent extraction of measurements from the profile, the best-fitting plane where the 3-D profile lies is determined, and the 2-D projection of the profile on this plane is evaluated and considered for the measurement phase.

D. Measurement Extraction

Two main steps [5], [6] are run to create a measurement procedure that is valid for all the profiles produced and that can also account for future production as well as be easily customized on the basis of the lengths to be monitored.

1) The observed profile of each profile piece is superimposed ("registered") onto the corresponding reference profile for comparison purposes [17], [18].
2) The dimensions to be measured are specified on the coordinate system of the reference profile and then are located and measured on the observed profile.

The reference profiles and the geometrical definitions of the lengths to be measured are stored in an ad hoc database. This archive can be upgraded by the user through a specific software module of the developed application called the "Profile Editor."

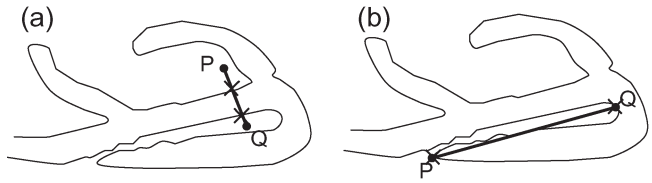

Fig. 5. Measurement primitives. (a) Gauge. (b) Tip-to-tip.

This module lets the user place measurement tools onto a reference profile, choosing them from a set of measurement primitives. Two types of measurement primitives have been introduced, i.e., the "gauge" [measurement of the distance between the two intersections of a specified segment and the observed profile, as shown in Fig. 5(a)] and the so-called "tip-to-tip" [the points with a maximum in the contour curvature best corresponding to those specified are located on the observed profile, and their distance is returned, as shown in Fig. 5(b)]. The latter could be either projected onto an axis specified using the Profile Editor or not.

E. Quality Test

Each measurement result is compared with the specification limits to assess its compliance with design tolerances, and the software reports the outcome of the dimensional test with a "pass/fail" indication. The reference values of each length to be measured and its specification limits are stored in the database using the "Profile Editor." Both the design tolerance and the measurement uncertainty have to be taken into account for this test.

The presentation of the results includes, for each piece, the superimposition of the observed and reference profiles, the table of last results, the time chart of the results, and some statistics. A screenshot of the software is shown in Fig. 6.

III. Metrological Characterization—Sources of Bias and Uncertainty

The metrological characterization of a measurement system first requires that the potential systematic effects, uncertainty sources, and influence parameters be identified and, then, that the sensitivity to these causes of uncertainty be evaluated. The metrological characterization was achieved with reference to the blocks described in Section II.

A. Image Acquisition

Several causes of errors are known for the localization of features in an image taken by a digital camera. The optical lens may introduce nonlinearity (distortion) that causes an imperfect matching of the common linear model with the actual acquired image, and the limited size of its aperture introduces a spreading of the size of the image of a point object due to diffraction. The sensing device of the camera imposes further constraints to both the spatial resolution and the intensity resolution of the image, and its differences from the ideal, such as skewness and variability in the size of pixel sensing areas or sensitivity, are also sources of systematic bias. The sensor thermal noise may also introduce random effects on the localization of image

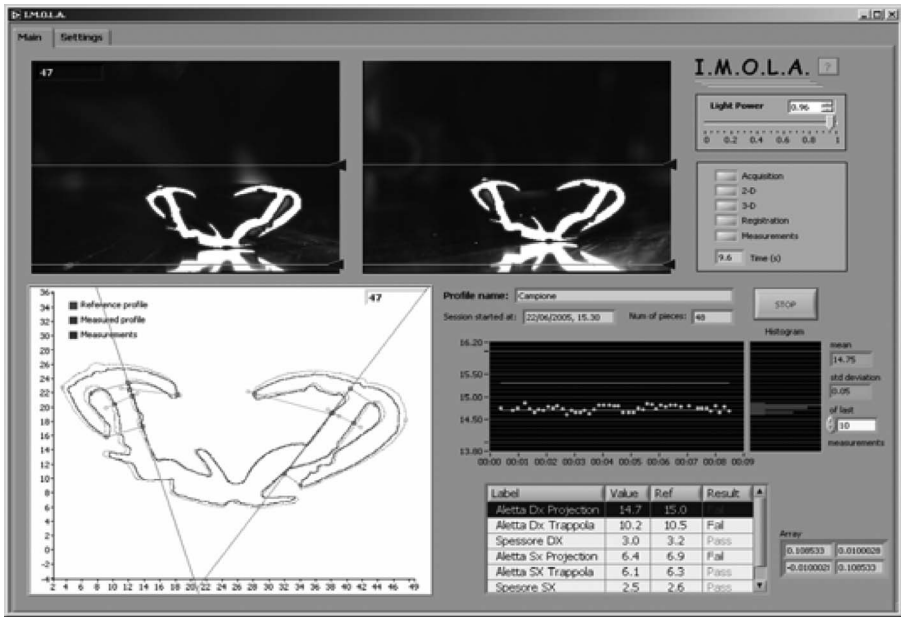

Fig. 6. Screenshot of the online application.

features. In the application setup, specific tests were made to establish that the effects of lens distortion and diffraction and of sensor skewness are negligible if compared with the effects of both the finite spatial and intensity resolutions of the image.

Another class of causes of uncertainty can be found within the environment. In the industrial environment, the main causes of image uncertainty are the flicker of light sources due, for instance, to the instability of the line power supply and the vibration of the object or of the cameras. It was impossible to avoid a certain level of vibration for the application setup due both to the cameras and to the object under measurement. On the other hand, environmental illumination was partially masked with opaque panels. The effects of image uncertainty on the measurement results also depend on a number of influencing factors such as the location of the object within the calibration volume and its relative position between the cameras.

It has to be underlined that the object position during the online operation cannot be fixed but only limited within a calibrated volume. The variation of the position of the objects under measurement introduces changes to the appearance of the object in both images and is then a cause of uncertainty.

B. 2-D Image Processing

The uncertainty of the acquired image propagates through the image-processing algorithms, determining uncertainty on the detected contours [11], [12]. The uncertainty of the edge position depends not only on the input image uncertainty but also on the image contrast and on the kind of edge. Furthermore, some profiles are made of different rubber compounds, and some types have a reinforcing metal structure. The illumination subsystem plays a critical role in these cases since the interface between different compounds may appear as an actual contour. Furthermore, the illumination intensity has an impact on edge uncertainty, and its effects could be different according to the kind of rubber used in the processed profile.

C. 3-D Reconstruction

The 3-D coordinate uncertainty of the reconstructed profile points depends not only on the 2-D coordinate uncertainty of the profiles determined in both images but also on the calibration parameter uncertainty.

The calibration phase is of fundamental importance for reconstruction accuracy since it defines the parameters for the 2-D–3-D transformation: inaccurate calibration parameter values determine incorrect reconstruction and, consequently, incorrect measurements. For a calibrated system, if some geometrical parameters such as camera positions, focus, etc., accidentally change, then the system becomes uncalibrated. A suitable procedure was defined to let operators verify that the system is calibrated, and, consequently, to verify that no further systematic errors are introduced in the 3-D reconstruction.

D. Measurement Extraction

The measurement process may introduce systematic and random effects due to both the registration phase and the measurement extraction. The quality of the registration results is summarized using a single parameter evaluated as the average of the distances between each point of the reconstructed profile and the closest point of the reference profile ["average minimum distance" (AMD)].

On the other hand, the uncertainty related to the measurement-extraction phase depends on different causes, i.e., the quality of the registration, the type of measurement primitive, and the localization of the length to be measured along the profile. The type of primitive is important since, for "tip-to-tip" measurements, the localization of the extremes is made with a different criterion, and its uncertainty is strongly dependent on the local shape of the profile. Moreover, if the "tip-to-tip" measurement has to be projected onto an axis, the uncertainty depends on the localization of the axis as well.

E. Quality Test

The final result of the automatic system is profile classification by means of a pass/fail test on all the measured lengths. The test requires a comparison between the measured value and the corresponding specification limits. Because of the uncertainty of the measured values, the comparison cannot be carried out as a simple comparison between the values. In fact, even if the measured value falls within the specification band, there is a nonzero probability that the value of the measurand is outside the specification range. It is possible to quantify the test result reliability in terms of pass/fail [10] and to make a decision on the basis of the evaluated reliability, which is expressed in terms of the confidence level evaluated as follows. Let x_0 be the measurement result, and let u_x be its uncertainty. x_0 and u_x can be considered, respectively, as the mean and standard deviation of the probability density function (pdf) $f_X(x)$ of the random variable X describing the measurement. If x_0 is used in a quality test, it has to be compared with the specification limits [lower specification limit (LSL) and upper specification limit (USL)] as

$$\text{Quality Test}: \qquad \text{LSL} < x_0 < \text{USL}.$$

The reliability of the condition "the value of the measurand complies with the specifications," hereinafter called PASS result confidence level or CL(PASS), can easily be estimated by considering the probability associated with the eventuality of the random variable being in the LSL $< X <$ USL [19] tolerance band

$$\begin{aligned}\text{CL(PASS)} &= P(\text{LSL} < X < \text{USL}) \\ &= \int_{\text{LSL}}^{\text{USL}} f(x)\,dx \\ &= F_x(\text{USL}) - F_x(\text{LSL}) \end{aligned} \tag{1}$$

where $F_X(x)$ is the cumulative distribution function of X.

Analogously, the confidence level of a FAIL result CL(FAIL) is equal to the probability associated with the eventuality of the random variable not being in the $X <$ LSL or $X >$ USL tolerance band

$$\begin{aligned}\text{CL(FAIL)} &= P(X < \text{LSL or } X > \text{USL}) \\ &= \int_{-\infty}^{\text{LSL}} f(x)\,dx + \int_{\text{USL}}^{\infty} f(x)\,dx \\ &= 1 - \text{CL(PASS)}. \end{aligned} \tag{2}$$

The confidence level of the PASS condition (see Fig. 7) CL(PASS) earlier calculated is adopted to classify the geometrical quantity of interest.

IV. Metrological Characterization—Experimental Results

A. Data Acquisition

Tests were carried out to evaluate the influence of the data-acquisition conditions on the measurements and to choose the best camera configuration. The experiments were performed by adopting three metallic gauge blocks (15 × 15 mm, 15 × 30 mm, and 30 × 30 mm, with an accuracy of less than 1 μm) as reference objects. These blocks are widely used as standard references in mechanical measurements, and in this case, they allow one to avoid considering the influence of shape cross section complexity upon the measurement results. In particular, given an object and having defined a number of vertical and horizontal lengths to be measured on it [as shown in Fig. 8(a)], a set of repeated measurements of each length was carried out in different poses of the object within the calibration volume.

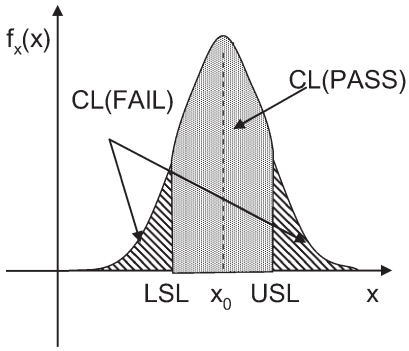

Fig. 7. Evaluation of the pass/fail test reliability in terms of confidence level.

A first series of tests was carried out to find the relative positions of the two cameras and of the object, thereby assuring a sufficient calibrated volume and an adequate accuracy.

The camera axis angles (α and β) and the baseline B are defined in Fig. 8(b). The values of α, β, and B reported in Table I were adopted for the tests. For each camera configuration, the following tests were carried out: 20 runs of the online processing procedure for each of the five different positions of the object in the calibration volume (center, left, right, center right, and center left). For each object, three geometrical measurements were defined (three heights and three widths). These sets of measurements were repeated for the three reference objects. An overall of 1200 measurements (four geometrical quantities × 20 repetitions × five positions × three objects) for each camera orientation were made. Table I reports the mean values, maximum values, and standard deviations of the measurement errors on the six defined lengths estimated by running the whole application for each camera configuration ("Conf"). Configuration no. 7, showing the lowest maximum error and standard deviation, was chosen as the definitive operating configuration in the proposed measurement system. With reference to Fig. 8(b), the calibrated volume for this configuration has a width w of 80 mm, a depth d of 40 mm, a height h of 80 mm, and a working distance WD of 280 mm.

B. 2-D Image Processing

To evaluate the variability of the localization of the 2-D contour, a rubber profile is kept in the same position during the acquisition and processing of 100 pairs of images (and the test was repeated for five different poses and for three different types of profiles). A 2-D histogram matrix was built with the same size as the images and whose (i, j) element values are equal to the number of occurrences of an edge at pixel (i, j) in

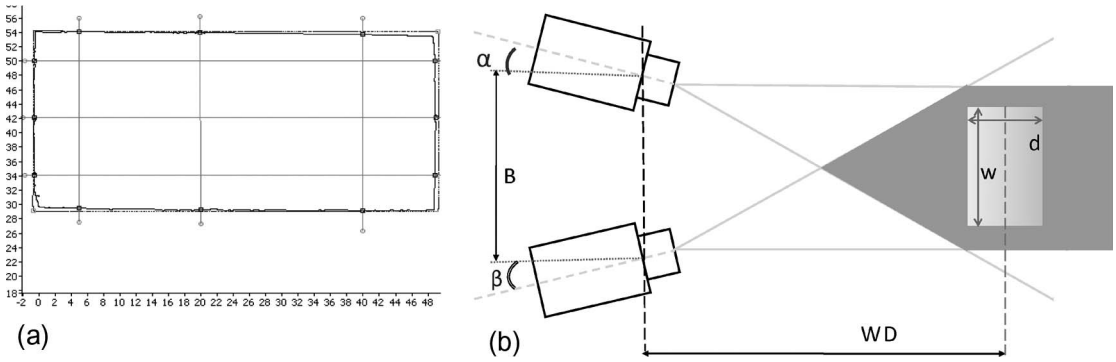

Fig. 8. (a) Dimensional measurements on gauge blocks. (b) Configurations of cameras and calibrated volume.

TABLE I
CONSIDERED CONFIGURATIONS AND CORRESPONDING RESULTS

Conf	α	β	B (mm)	Mean Error (mm)	Max Error (mm)	Dev.St (mm)
1	0º	15º	120	0.037	0.438	0.239
2	0º	12º	120	-0.240	0.911	0.302
3	0º	18º	120	-0.028	1.041	0.146
4	7º	7º	115	0.048	0.946	0.210
5	10º	10º	164	0.146	1.410	0.145
6	17º	17º	190	0.296	1.033	0.312
7	2º	13º	120	-0.062	0.255	0.079

the 100 images. The results show that the edge positions were always within ± 1 pixel from the most frequent position for each kind of profile and in all the exploited positions. Generally, the edge is detected in the same position in more than 85% of the cases; otherwise, it is localized in one of the two adjacent pixels. Only for a very few points, which are positioned close to the high curvature edge points, is a bigger dispersion observed; the central position is characterized by a lower frequency, i.e., nearly 60%, whereas the two adjacent pixels are characterized by a higher frequency.

C. 3-D Reconstruction

An important tool for plant operators is a metrological performance test to be periodically run to establish if either a new calibration is necessary or the available calibration data are still valid. This performance test uses a target similar to that used in the calibration (see Fig. 3) and verifies the planarity of the reconstructed 3-D contour points and the length measurement errors of the square holes. To evaluate the bounds of both the nonlinearity and the dimensional errors, repeated measurements were carried out in the case of a calibrated system, running ten repeated calibrations, and placing a test target with 3 mm $\times$ 3 mm square holes in five different positions in the calibrated area. The images are processed, and the edges of the square holes of the target are localized in 3-D space. Then, the least-square fitting plane is evaluated, the distances between the points and the plane are calculated, and the hole dimensions and their mutual distances are estimated (Fig. 9). In these experiments, it was observed that the dimension test is more significant than the planarity test. In particular, the average of the distances from the interpolated plane is always less than 0.15 mm, whereas the standard deviation of the distances is less than 0.25 mm. However, for small modifications of the

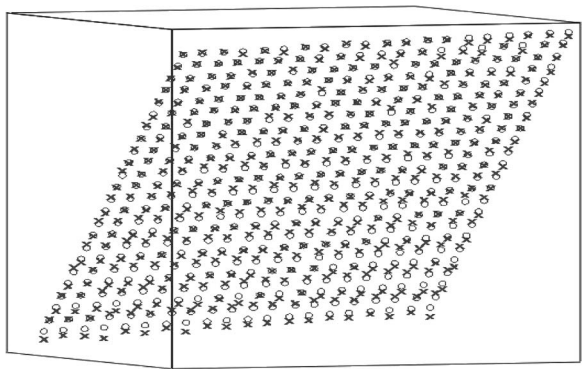

Fig. 9. Comparison between the measured vertices of the target and the reference ones.

camera system, these values are still warranted, and greater values are measured only for relevant changes. On the other hand, the nominal dimensions and distances are equal to 3 mm, the mean of all the measured quantities is always within $3.000 \text{ mm} \pm 4 * 0.0179$ mm, and even the smallest changes cause the mean values to fall out of the interval.

D. Measurement Extraction

The first step of the measurement phase is the registration of the observed profile onto the reference profile. The algorithm minimizes the average of the distances between each point of a profile and the closest point of the other. The value of the AMD is used as an indicator of the correctness of the registration. The typical values of this parameter in operating conditions are on the order of 0.3 mm.

The next step to be characterized is measurement extraction. To determine possible systematic effects, repeated measurements were carried out on metallic objects: 1) on the 25 $\times$ 50 mm reference gauge block and 2) on a bar whose cross section reproduces that of a rubber profile. Other tests were carried out 3) on the actual rubber profiles.

1) The reference gauge block was placed in three different positions in the calibrated area, and for each position, the online processing procedure was run 20 times. The system is configured to perform three height and three width measurements, thereby obtaining 180 horizontal and 180 vertical geometrical measurements overall. A statistical analysis is carried out on these results to

TABLE II
RESULTS OF THE EVALUATION OF CORRECTION FACTORS

Horizontal				
W_{meas}	W_n	s_{Wmeas}	Cw	u_{Cw}
49.35 mm	50.00 mm	0.08 mm	1.013	0.002
Vertical				
H_{meas}	H_n	s_{Wmeas}	C_H	u_{CH}
24.57 mm	25.00 mm	0.03 mm	1.017	0.002

estimate systematic errors and, consequently, to calculate the correction factors, together with their uncertainties.

The horizontal and vertical correction factors C_W and C_H, respectively, were calculated using the reference values W_n and H_n, and the measured average values along the two directions, respectively, W_{meas} and H_{meas}, i.e.,

$$C_H = \frac{H_n}{H_{\text{meas}}} \quad , C_W = \frac{W_n}{W_{\text{meas}}}. \tag{3}$$

The correction factor uncertainties are evaluated as

$$u_{C_H} = C_H \frac{\sigma^*_{H_{\text{meas}}}}{H_{\text{meas}}} \quad , u_{C_W} = C_W \frac{\sigma^*_{W_{\text{meas}}}}{W_{\text{meas}}} \tag{4}$$

where σ^* stands for the standard deviation of the mean corresponding quantity. The correction factors achieved, shown in Table II, are stored in a file and are loaded and applied by the measurement procedure during normal operation.

2) The metallic profile was adopted since it can be measured both by the proposed system as an ordinary rubber profile and by an accurate contact measurement system, thus allowing a comparison of the results to be achieved by the image-based measurement system. For each object, a set of contours of the nominal section was accurately edited by CAD operators (to be used as a reference profile during the registration and measurement phases of the software application). Seven different measurements were defined and placed on the reference profile so that possible influence quantities are highlighted (see Fig. 10). For example, measurement L_1 evaluates the length of a segment between the end and the base of a tongue, projected onto an axis placed on the left part of the section. For a statistical analysis, the metallic profile was manually placed in 30 different positions within the calibration area, and for each position, the online processing procedure was run.

   Table III summarizes the results of these tests in terms of mean and standard deviation of the errors for each geometrical measurement. Negligible residual systematic effects are observed, and the standard deviations of the measured values are always less than 0.15 mm, except for the measurement L_4, where a higher value is measured. The results obtained with the other types of profiles agree with those in Table III.

   Considering both the standard deviations and the residual errors, it is possible to assign a value to the uncertainty of each measurement on the basis of the applied primitive. For the tip-to-tip primitive with the projection onto an axis, the assigned uncertainty is 0.10 mm. For the tip-to-tip primitive without projection, the assigned uncertainty is 0.15 mm. For the gauge primitive, an uncertainty of 0.08 is assigned.

3) Experimental measurements were carried out using an actual rubber profile to evaluate the uncertainty of the whole measurement system and to take into account all the considered uncertainty sources. The profile was repeatedly positioned on the conveyor belt 30 times, and the online processing procedure was run each time. The results for the rubber profile are summarized in Table IV. In this case, reference values are not reported since, on a rubber profile, contact measurement devices cannot be used, and other measurement methods (such as those adopting a magnifying projector) have uncertainty comparable or worse than the system under characterization. These results, together with others carried out on other profiles, are substantially similar and confirm the three classes of uncertainty previously introduced.

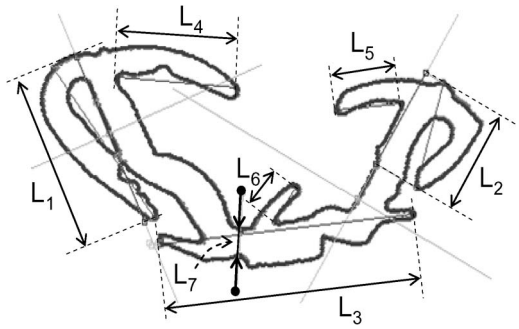

Fig. 10. Definition of the lengths to be measured on the reference profile.

E. Quality Test

To establish confidence level conformity, a number tests were carried out. First, for each of the lengths monitored, data were collected to estimate the *pdf* that describes its variability. Then, on the basis of both the pdf and the tolerance, the trends of CL(PASS) versus the measured values were calculated. Finally, using this last relationship, new limits that assure a given CL are defined.

The measurement *pdfs* were estimated using the measurement results in Section IV-D (list item 3). In particular, the collected data were also used to carry out a chi-square test with different distributions. The results showed that the best model is a Gaussian distribution since the chi-square values are nearly always less than 5.58, which is the limit value with $\alpha = 0.9$ when using a number of classes equal to 12.

In Fig. 11, the trends of CL(PASS) versus the measured values of length L_3 are shown together with a cut line for the CL value of 0.9. The interval of the measured values with a CL(PASS) value greater than 0.9 (namely the acceptance interval) can be estimated, giving the new limits, as required by the quality laboratory. For length L_3 of the example, we have an uncertainty equal to 0.15 mm, a nominal value of 25.00 mm, a tolerance of 0.50 mm, a lower limit of 24.64 mm, and higher limit of 25.36 mm.

TABLE III
RESULTS FOR THE METALLIC OBJECT ON THE LENGTHS DEFINED IN FIG. 10. ALL MEASUREMENTS ARE IN MILLIMETERS

Measurement	Type	Reference Value	$\bar{x}$	Error	s_x
L_1	Tip-to-tip + proj.	17.100	17.149	0.049	0.082
L_2	Tip-to-tip + proj	10.000	9.920	-0.080	0.090
L_3	Tip-to-tip	25.000	24.955	-0.045	0.094
L_4	Tip-to-tip	11.650	11.600	-0.050	0.130
L_5	Tip-to-tip	6.350	6.335	-0.165	0.072
L_6	Tip-to-tip	3.900	3.964	0.064	0.035
L_7	Gauge	2.500	2.559	0.059	0.068

TABLE IV
RESULTS FOR A RUBBER PROFILE WITH THE NOMINAL SECTION OF FIG. 10

Measurement	Type	$\bar{x}$ [mm]	s_x[mm]
L_1	Tip-to-tip + proj.	16.973	0.090
L_2	Tip-to-tip + proj	9.100	0.083
L_3	Tip-to-tip	24.787	0.138
L_4	Tip-to-tip	11.148	0.120
L_5	Tip-to-tip	5.656	0.135
L_6	Tip-to-tip	3.476	0.097
L_7	Gauge	2.892	0.064

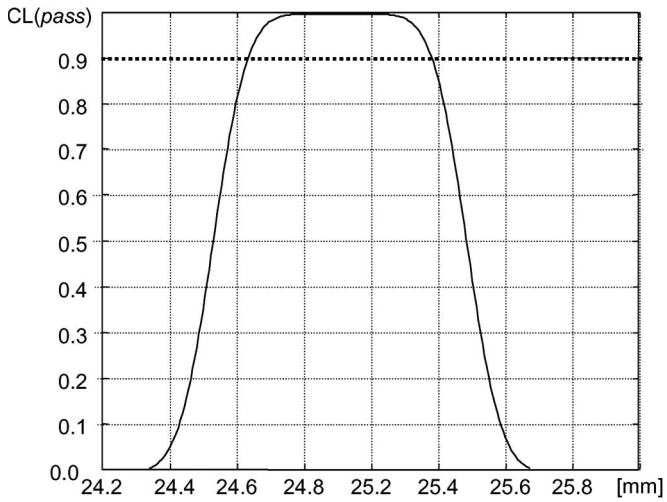

Fig. 11. CL trends for the measurements of lengths L_3. The cut line at CL $= 0.9$ is shown.

V. CONCLUSION

The metrological characterization of a stereovision-based measurement system for the online inspection of automotive rubber profiles has been presented. The first aim of the metrological characterization was to identify potential systematic effects, uncertainty sources, and influence parameters with reference to the single blocks that comprise the system. All the causes of uncertainty were then separately analyzed, where possible. In addition, the total measurement uncertainty was evaluated. The methods used can be applied to the characterization of other vision-based measurement systems since they share similar issues.

Due to the correction of systematic effects and the optimized choice of the system configuration parameters, the whole measurement uncertainty is less than 0.2 mm. Moreover, the value of the uncertainty is used in the quality control activities to estimate the reliability of an automatic classification of geometrical measurements as "compliant" or "not compliant." In particular, the confidence level of the statement "the value of the length complies with design tolerances" is evaluated on the basis of the measurement distribution and measured value. If it is greater than 0.9, a "pass" indication is associated with the measurement results; otherwise, a "fail" warning is displayed in correspondence to the measurement.

The proposed system is currently operating on the production lines at a Metzeler APS plant. The achieved performances meet the requirements for the quality inspection of these types of rubber products, and the value of the minimum confidence level for a "pass" classification was established on the basis of the maximum acceptable level risk.

ACKNOWLEDGMENT

The authors would like to thank Prof. A. Pietrosanto for the very useful suggestions given in designing the measurement system and in analyzing the causes of uncertainty.

REFERENCES

[1] A. M. Wallace, "Industrial applications of computer vision since 1982," *Proc. Inst. Elect. Eng.—Comput. Digit. Tech.*, vol. 135, no. 3, pp. 117–136, May 1988.
[2] Y. Sumi, M. Sallinen, M. Sirvio, and J. Vainola, "Recognition of large work objects in difficult industrial environments," in *Proc. IEEE Int. Conf. Syst., Man Cybern.*, 2004, vol. 6, pp. 5285–5289.
[3] L. Angrisani, P. Daponte, A. Pietrosanto, and C. Liguori, "An image-based measurement system for the characterization of automotive gaskets," *Meas.*, vol. 25, no. 3, pp. 169–181, 1999.
[4] C. Liguori, A. Paolillo, and A. Pietrosanto, "An online stereo-vision system for dimensional measurements of rubber extrusions," *Meas.*, vol. 35, no. 3, pp. 221–231, Apr. 2004.
[5] R. Anchini, G. Di Leo, C. Liguori, and A. Paolillo, "New measurement techniques for the on line dimension characterization of automotive rubber profiles," in *Proc. 18th IMEKO World Congr., Metrology Sustain. Dev.*, Rio de Janeiro, Brazil, Sep. 2006.
[6] R. Anchini, G. Di Leo, C. Liguori, and A. Paolillo, "Metrological characterization of a vision-based measurement system for the online inspection of automotive rubber profile," in *Proc. IEEE Workshop AMUEM*, Trento, Italy, Jul. 2007, pp. 121–126.
[7] J. J. Aguilar, F. Torres, and M. A. Lope, "Stereo vision for 3D measurement: Accuracy analysis, calibration and industrial applications," *Meas.*, vol. 18, no. 4, pp. 193–200, Aug. 1996.

[8] D. Torkar and G. Papa, "Accuracy of a 3D reconstruction system," in *Proc. 6th WSEAS Int. Conf. Signal Process. Robot. Autom.*, Corfu Island, Greece, Feb. 2007, pp. 146–150.
[9] *VDI/VDE 2634 blatt 2, optische 3D-messsysteme—Systeme mit flächenhafter antastung/optical 3-D measuring systems—Optical systems based on area scanning*, Aug. 2002.
[10] OIML, *Guide to the expression of uncertainty in measurement*, 1995.
[11] M. De Santo, C. Liguori, A. Paolillo, and A. Pietrosanto, "Standard uncertainty evaluation in image-based measurements," *Meas.*, vol. 36, no. 3/4, pp. 347–358, Oct.–Dec. 2004.
[12] R. Anchini, C. Liguori, and A. Paolillo, "Evaluation of the uncertainty of edge detector algorithms," in *Proc. IEEE Int. Workshop Adv. Methods Uncertainty Estimation Meas.*, Sardagna, Italy, Apr. 20–21, 2006, pp. 68–73.
[13] R. C. Gonzalez and R. E. Woods, *Digital Image Processing*, 2nd ed. Upper Saddle River, NJ: Prentice–Hall, 2002.
[14] R. Jain, R. Kasturi, and B. G Schunck, *Machine Vision*. New York: McGraw-Hill.
[15] Z. Zhang, "A flexible new technique for camera calibration," Microsoft Res., Redmond, WA, Tech. Rep. MSR-TR-98-71, 2002.
[16] O. Faugeras, *Three-Dimensional Computer Vision*. Cambridge, MA: MIT Press, 1993.
[17] "Iterative point matching for registration of free-form curves and surfaces," *Int. J. Comput. Vis.*, vol. 13, no. 2, pp. 119–152, Oct. 1994.
[18] A. Bovik, Ed., *Handbook of Image and Video Processing*, 2nd ed. New York: Academic, 2005.
[19] G. Betta, C. Liguori, and A. Pietrosanto, "Uncertainty evaluation in algorithms with conditional statement," *IEEE Trans. Instrum. Meas.*, vol. 53, no. 4, pp. 969–976, Aug. 2004.

Rosario Anchini was born in Salerno, Italy, in 1976. He received the M.S. degree in electronic engineering in 2003 from the University of Salerno, where he is currently working toward the Ph.D. degree in information engineering.

His current research interest is concerned with systems for noncontact measurement based on image processing. In particular, his attention is focused on their metrological characterization with the aim to provide analytical methods to predict the uncertainty of the results of such systems.

Giuseppe Di Leo was born in Sarno, Italy, in 1972. He received the M.S. degree in electronic engineering in 2001 from the University of Salerno, Salerno, Italy, where he is currently working toward the Ph.D. degree.

Since 2002, he has been with the Department of Electrical and Information Engineering (DIIIE), University of Salerno. He has coauthored papers in national and international conference proceedings. His main research activities are in the field of metrological characterization of measurement systems, image-based measurement systems, and digital signal processing.

Consolatina Liguori (M'99) was born in Solofra, Italy, in 1969. She received the M.S. degree in electronic engineering from the University of Salerno, Salerno, Italy, in 1993 and the Ph.D. degree from the University of Cassino, Cassino, Italy, in 1997.

In 1997, she was an Assistant Professor of electrical measurements with the Department of Industrial Engineering, University of Cassino. Since 2001, she has been with the University of Salerno, where she was an Associate Professor of electrical and electronic measurements, and has been with the Department of Information Engineering and Applied Mathematics since 2004. Her main interests are in fields of digital signal processing and image-based measurement systems, measurement characterization, and instrument fault detection and isolation.

Alfredo Paolillo (M'08) was born in Belvedere M.mo, Italy, in 1972. He received the M.S. degree in electronic engineering from the University of Salerno, Salerno, Italy, in 2000. He is currently working toward the Ph.D. degree in information engineering with the Department of Information and Electrical Engineering (DIIIE), University of Salerno.

Since 2002, he has been an Assistant Professor of electrical and electronic measurements with the University of Salerno. His research activities include optical fiber temperature sensors, image-based measurement systems, and digital signal processing.